New Insights on the Photodissociation of *N*-Methylpyrrole: The Role of Stereoelectronic Effects†

Giovanni Piani,† Luis Rubio-Lago,†,‡ Martin A. Collier,† Theofanis N. Kitsopoulos,‡,¶ and Maurizio Becucci*,†,§

European Laboratory for Non-linear Spectroscopy, Sesto Fiorentino (Firenze), Italy; IESL-FORTH, Heraklion, Greece, Department of Chemistry, University of Creete, Greece; and Department of Chemistry, Università di Firenze, Italy

Received: April 30, 2009; Revised Manuscript Received: September 15, 2009

We investigated the reaction dynamics of *N*-methylpyrrole (NMP) along the N−CH_3 coordinate, upon excitation energies below 6.4 eV. Ours and previous experiments show clearly the existence of different reaction channels leading to slow and fast fragment production whose relative efficiency fluctuates with the changes in the excitation energy. Thanks to our modeling based on the differences of the NMP molecular orbitals (MOs) with respect to those of pyrrole we are able to show the existence of two low lying dissociative $\pi\sigma^*_{N-CH_3}$ states. Those states originate from the degeneracy removal in the π MOs owing to their interaction with the σ_{CH} MO of the methyl group. This evidence and the calculated potential energy surfaces for dissociation along the N−CH_3 coordinate provide the correct framework for the interpretation of the details in the NMP photodissociation dynamics.

Introduction

Pyrrole and its derivatives are prototypical six π-electrons aromatic molecules, and can be used as ideal models for the study of more complex systems like nucleobases and aromatic aminoacids. They also play a key role in synthesis of biologically active compounds, polymers, and organometallic complexes. Several research papers have been published on the photodissociation of this class of compounds, pointing out the role of a $\pi\sigma^*_{N-X}$ dissociative state (along the N-X bond) as a decay channel for the photoexcited pyrrole and subsituted pyrroles. In particular the photodissociation dynamics of pyrrole and 2,5-dimethylpyrrole are well-known;[1,2] the experimental evidence of the presence of two dissociation channels producing slow and fast H fragments has been explained with the possibility of two different mechanisms: the first is a statistical dissociation via internal conversion (IC) to the ground states; the second is a direct dissociation via $\pi\sigma^*_{N-H}$ state, as also recognized in other hydride heteroatomic molecules. Production of slow H-atoms upon photoexcitation of *N*-methylpyrrole (NMP) has also been reported,[3] suggesting that IC plays a role in the excited state decay. It is also a clear indication that the N−H cleavage should be not the only source of H atoms for excited pyrrole.

To obtain more information on the $\pi\sigma^*_{N-X}$ dissociation channel, research was focused on the NMP molecule. The position of methyl radical in NMP is equivalent to the position of the H atom bonded to nitrogen in pyrrole, and thus the N−CH_3 bond is supposed to play a similar role in the NMP photodissociation as the N−H bond in the case of pyrrole: the first evidence of the direct detection of CH_3 dissociating from NMP supports this hypothesis.[4] Furthermore, N−CH_3 cleavage is the only possible source of methyl fragments in NMP, so we are selectively studying the dissociation along the N−X reaction coordinate.

Very recently two reports have been published on the UV photodissociation of NMP. In the first, Sage et al. studied the UV photodissociation of NMP in the range 243−225 nm obtained by REMPI and velocity mapping−ion imaging techniques.[4] Two reaction channels were reported leading to slow or fast CH_3 radical production. The slow channel was observed for all the excitation wavelengths used in the experiment. The fast channel was active only in a very narrow wavelength range close to the origin band of the electronic absorption spectrum. These two channels were attributed to dissociation processes taking place in the electronic ground state or in the electronic excited state, respectively. In the second report, the photodissociation of different methyl-substituted aromatic compounds was experimentally studied upon excitation at 248 and 193 nm by Tseng et al., using a multimass ion imaging technique.[5] The electronic excited states of NMP were directly accessible only for 193 nm excitation. The production of slow CH_3 fragment was demonstrated as the dominant process. Fast fragments were observed, too, even if with very low quantum yield. As it was noticed in the two papers, calculations of the potential energy surfaces for excited states of NMP are not present in literature.

We have become interested in the problem of NMP photodissociation, mainly the intriguing question of the changes in the reported production of fast CH_3 fragments, and we have tried to provide new information in two ways. First, we conducted some experiments at different excitation energies, trying to fill the gap between the data available in the 243−225 nm range and those at 193 nm. We have also made new measurents at 193 nm, providing new details for the fast fragments channel observed at this excitation energy. Second, we have discussed the existence and relevance of different reaction channels leading to the production of fast CH_3 fragments. With the aim of providing some guidelines for the interpretation of the experimental results we have also performed

† Part of the "Vincenzo Aquilanti Festschrift".

* To whom correspondence should be addressed. E-mail: becucci@lens.unifi.it.

† European Laboratory for Non-linear Spectroscopy.

‡ IESL-FORTH.

¶ University of Creete.

§ Università di Firenze.

10.1021/jp903992u
Published on Web 10/14/2009

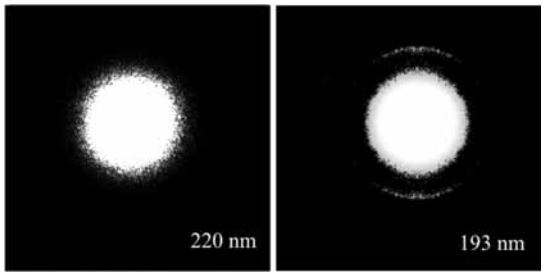

Figure 1. CH_3 fragments from NMP photodissociation upon 220 and 193 nm excitation (left and right panel, respectively). CH_3 ($v = 0$) fragments have been detected with REMPI schemes at 286.31 and 333.62 nm, respectively. The images are strongly saturated in order to show clearly the possible existence of fast CH_3 fragments. Laser radiation is polarized vertically in the same plane of the images.

TD-DFT calculations for the evaluation of the number and nature of the excited states possibly involved in this photochemical process.

Experimental Methods

We have performed single field slice ion imaging experiments, both at LENS and FORTH. Regarding the experimental apparatus at FORTH, it is already described elsewhere.[6] The one at LENS was recently built and closely resembles the one at FORTH.

Laser radiation for NMP excitation was provided by excimer lasers (193 nm) and by frequency doubled dye lasers (between 225 and 210 nm; BBO crystals used for harmonic generation start absorbing below 210 nm, so lower wavelengths are not accessible using this experimental setup). The CH_3 fragments produced in their ground vibrational state were selectively ionized thanks to multiphoton excitation schemes using radiation either at 333.62 or 286.31 nm wavelength (from frequency doubled dye lasers).

NMP has been purchased by Aldrich and used without purification. The carrier gas was helium, and the backing pressure was set at ~1 bar.

The calibration of the kinetic energy release for the fragments produced was done using results from the photodissociation of CH_3Br.[7]

Results

Experimental Results. Previous studies covered the excitation range between 243 (the origin of the singlet electronic absorption spectrum of NMP) and 225 nm[4] while at higher energies a single experiment was performed (at 193 nm excitation).[5] We have provided new data on the photodissociation of NMP along the N−CH_3 coordinate in the region between 225 and 210 nm excitation using tunable dye lasers. Results have been very similar for all these new measurements, showing only a broad, structureless, central feature with an intensity distribution that decreases monotonically from the center to the external region. To provide a common ground between all the experimental evidence, as the published results at 193 nm were not presenting an extended discussion on the TKER upon photodissociation, we have repeated the photodissociation experiment at 193 nm, and the result shows the same dynamics already reported by Tseng et al.[5]

Figure 1 shows the CH_3 ion images resulting from experiments with 220 and 193 nm excitation of NMP (left and right panel, respectively). Both images are strongly saturated in order to show more clearly the possible presence of fast fragments.

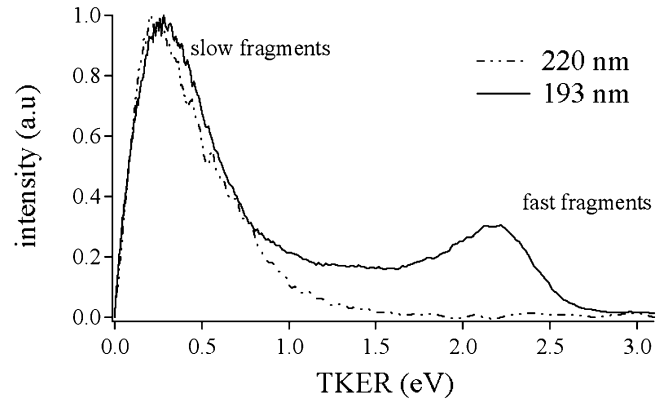

Figure 2. TKER for the fragments produced by photodissociation of NMP at 220 and 193 nm. The data were elaborated from saturated images in order to emphasize the contribution from weak signals therefore the contribution for the fast channel is strongly enhanced.

Standard methods were applied to measure the kinetic energy of the CH_3 fragment from the different images. The total kinetic energy release (TKER) was determined by simply applying the formula

$$\mathrm{TKER} = \frac{m_{\mathrm{NMP}}}{m_{\mathrm{C_4H_4N}}}\mathrm{KER}_{\mathrm{CH_3}} \quad (1)$$

From the analysis of the unsaturated images, the production of slow fragments has a distribution of TKER centered around 0.2 eV and is angularly isotropic, for all the different excitation conditions. The production of fast fragments, observed in our data only upon 193 nm excitation, has a rather broad distribution of TKER that shows a peak around 2.1 eV and is partially anisotropic, as clearly shown in Figure 1. The translational energy spectrum for the fragments produced upon photodissociation of NMP at 220 and 193 nm is reported in Figure 2. To show more clearly the lack (or presence) of fast fragments, the data handling process resulted in a distortion of the shape of the low energy TKER profile.

The anisotropy for the fast fragments distribution under 193 nm excitation was never reported. We have fitted our data with the usual function:

$$I(\theta) = \left(\frac{1}{4}\pi\right)[1 + \beta P_2(\cos\theta)] \quad (2)$$

where $I(\theta)$ is the signal intensity in function of the angle formed by the light polarization axis and the velocity of the fragments (θ), β is the anisotropy parameter, and $P_2(\cos\theta) = {}^1/_2(3\cos^2\theta - 1)$ is the second order Legendre polynomial.[8] We are able to provide for β a value of 0.41(1), corresponding to a partially parallel transition.

TD-DFT Calculations. We have used a time dependent-density functional (TD-DFT) approach in order to evaluate the potential energy curves versus N−CH_3 distance, using the G03 package.[9]

First of all, we have optimized NMP structure at B3LYP/cc-pVDZ level of theory, obtaining a value of 1.4497 Å for the N−CH_3 distance in the equilibrium structure. Then, freezing this parameter to selected values, we have optimized, at the same theory level, the NMP ground state structure tracing thus the E_{pot} versus N−CH_3 distance curve in S_0. Finally, from each point in S_0 we have calcutated the vertical transitions leading to the

TABLE 1: Singlet Excited States of NMP: Nature of the Transition from the Ground State and the Corresponding Oscillator Strength as Derived from TD-B3LYP/cc-pVDZ Calculations Starting from the Equilibrium Geometry[a]

	state		$S_n \leftarrow S_0$ transition	f
S_1	A″	$\pi\pi^*$	π_4^* (LUMO) ← π_3 (HOMO)	0.0785
S_2	A″	$\pi\sigma^*$	σ^*_{N-CH3} (LUMO + 1) ← π_3 (HOMO)	0.0000
S_3	A″	$\pi\pi^*$	π_4^* (LUMO) ← π_2 (HOMO − 1)	0.0756
S_4	A″	$\pi\sigma^*$	σ^*_{N-CH3} (LUMO + 1) ← π_2 (HOMO − 1)	0.0074

[a] π MOs are labeled as in Figure 4. The states are classified by symmetry according to the C_s point group.

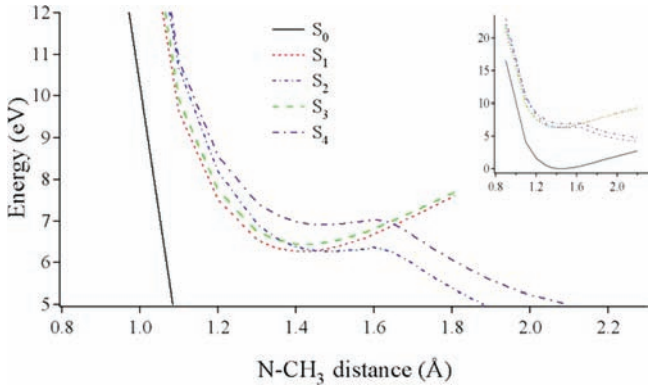

Figure 3. NMP potential energy curves (singlet states only) for the N−CH_3 bond elongation in NMP calculated at the TD-B3LYP/cc-pVDZ level of theory.

lowest singlet excited states, reconstructing in this way also the excited states potential curves for the N−CH_3 bond elongation.

In Table 1 we report the dominant character for the lowest singlet excited states and the molecular orbitals most involved in the corresponding transitions originating from the ground state. The result of this calculation are graphically shown in Figure 3 where, for a simpler reading, only the first four excited states (more relevant for our study) are presented.

TD-DFT calculations at this level of theory have a limited computational cost but present some limitations (B3LYP-DFT approach, the dimension of the basis set used, no inclusion of the zero point vibrational energy, etc.). Neverthless, given the complete experimental and theoretical study on pyrrole[1,10,11] and the detailed experimental data on NMP, even this evaluation of the potential surfaces involved in NMP dissociation can be quite effective for the description of the process.

However, to check the effect of increasing the basis set on the results, a calculation was made with triple ζ basis set

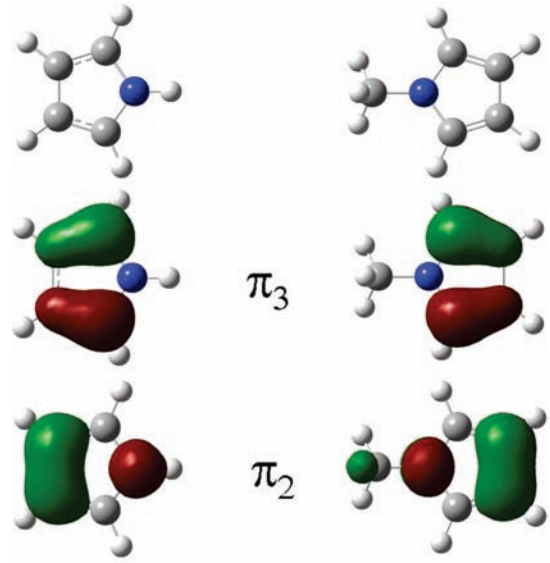

Figure 5. Electronic density maps of the highest π MOs of pyrrole and NMP.

(B3LYP/cc-pVTZ) at selected geometries. One of the observed effects is to make the energy gap between the ground and the first excited state much closer to the experimental data ($\Delta E_{double\zeta}$ = 6.3 eV, $\Delta E_{triple\zeta}$ = 5.9 eV, ΔE_{exp} = 5.1 eV).

It is possible that the actual assignment of the levels in NMP may be different with respect to that reported in Table 1 and Figure 3. The most questionable part is the exact character of the two lowest singlet electronically excited states as our calculations predict $\pi\pi^*$, as the S_1 state and $\pi\sigma^*$ as S_2 with a very small energy separation. The other assignments are very clear in TD-DFT calculation with both double ζ and triple ζ bases.

Discussion

In this section we will try to provide an unifying view for our data and all the existing data on the NMP photodissociation along the N−CH_3 coordinate upon excitation below 6.4 eV. We can summarize our's and previous[4,5,12−14] experimental evidence on the properties of electronically excited NMP as follows.

Spectroscopic studies are showing that the REMPI spectrum of NMP presents narrow bands very close to the origin of the $S_1 \leftarrow S_0$ bands. A diffuse background arises starting around 240 nm. It becomes a broad and relatively strong band between

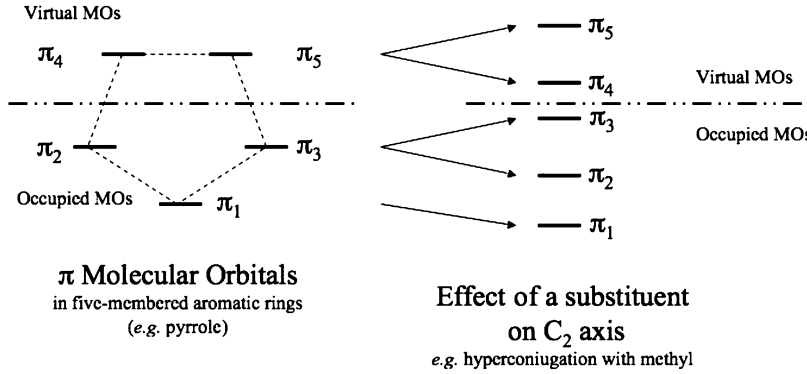

Figure 4. Energy diagram according to Hückel molecular orbital theory. Going from pyrrole to NMP, hyperconiugation between the aromatic ring and methyl substituent removes the degeneracy of the two highest π MOs. Exactly the same effect can be observed for the two π^* MOs. The electronic density maps of the highest π MOs are reported in Figure 5, both for pyrrole and NMP.

230 and 205 nm. Then, a very strong and broad absorption band starts around 200 nm.

With respect to reaction dynamics, slow CH_3 fragments are produced at all the different excitation energies investigated by Sage et al.,[4] Tseng et al.,[5] and in the present work, with a TKER around 0.2 eV. Fast CH_3 fragment production is reported only for excitation between the origin of the electronic absorption spectrum and +640 cm^{-1} (corresponding to the 243−239 nm range) and at 193 nm. No evidence is present for activity in the fast reaction channel in the excitation range of 238−210 nm. The fast fragments are produced with TKER of 0.8 eV in the case of excitation around 243 nm and 2.1 eV for 193 nm excitation.

Simple molecular orbital (MO) theory provides the basic keys for understanding the observed photodissociation on NMP in comparison to the known properties of pyrrole. The introduction of a methyl substituent on the nitrogen atom in pyrrole (leading to NMP) does not break the C_{2v} symmetry of the system: the methyl group is placed on the C_2 symmetry axis, the torsional barrier for the rotation around N−CH_3 bond is small,[14] and a free internal rotation can be assumed. As schematically shown in Figure 4, that follows the traditional Hückel theory for an aromatic molecule, the substituent removes the degeneracy of the two highest π MOs of pyrrole (and similarly of the two lowest π^* ones) due to stereoelectronic effects (hyperconiugation): the effective superimposition of the $\sigma_{CHmethyl}$ electron density with the π aromatic orbitals. At the same time, being no change in the effective symmetry, the substitution does not affect the selection rules for the electronic transition.

Fast H atoms during pyrrole photodissociation are produced because $\pi\pi^*$ excited molecules can reach the dissociative $\pi\sigma^*_{N-H}$ state.[11] Because of the degeneracy removal for the π MOs, in NMP we can expect two dissociative $\pi\sigma^*_{N-CH_3}$ reaction channels at relatively low energy, with initial electronic excitation starting from NMP π highest occupied molecular orbital (HOMO) or HOMO-1 (corresponding to the degenerate π HOMOs of pyrrole). At longer N−CH_3 distances the interaction between the methyl group and the aromatic ring is lost: therefore the energies of the two π orbitals converge to the same value, so the final state for the dissociation mechanism starting with excitation either from the HOMO or HOMO-1 NMP orbitals is the same.

According to our TD-DFT calculations on NMP, these two dissociative channels leading to the production of fragments in the same final quantum state exist and, at the ground state equilibrium distance, are separated by one bound states. Experimentally, we are able to locate this energy landscape in the 5.10−6.42 eV energy range (corresponding to the studied 243−193 nm photon excitation range). There are two features in the experimental results that strongly support this view. The first is the gap in the production of fast fragments in going from the origin of the electronic absorption spectrum and 193 nm: that is associated to the existence of two different dissociative states involved in the process. The second is the 1.3 eV TKER difference for the fast fragments produced with the 193 nm experiment and those produced with excitation at the origin of the NMP electronic absoption band: this energy difference matches the photon energy difference, as it should be expected for photodissociation processes producing fragments in the same final quantum state.

The excited states predicted by simple MO evaluations and TD-DFT calculations are providing a satisfactory interpretation for all the different features of the observed, in different stages, for NMP photodissociation along the N−CH_3 coordinate. The slow fragments production is a common feature for excitation of NMP at the different wavelengths and it is usually associated to the occurrence of the internal conversion (IC) process that allows excited molecules to reach vibrationally excited levels of the electronic ground state from which the breaking of the N−CH_3 bond is possible, typically with a small release of kinetic energy, as a statistical process. The fast fragments production around the origin of the electronic absorption band is related to the crossing between the bound $\pi\pi^*$ state (optically active) and the dissociative (dark) $\pi\sigma^*_{N-CH_3}$ state. Assuming as good the energy landscape obtained at the B3LYP/cc-pVDZ level of theory, as the N−CH_3 distance slightly increases from its equilibrium value the potential curve of the bound S_1 state is crossed by that of the dissociative S_2 state. It is then much more likely that molecules excited to the S_1 state can reach the N−CH_3 dissociative S_2 state of the same symmetry thanks to a process mediated by vibrations, leading then to the production of fast fragments.[4] This process, according to Sage et al. is still rather slow as an isotropic fragment distribution is observed.[4] That is in agreement with the small barrier to dissociation present at the S_2 surface at ∼1.6 Å, according to our calculations.

At some higher energy is located the S_3 state, an optically active, bound $\pi\pi^*$ state of the same symmetry of S_0 in the C_s point group. It is a state that can act as a very effective doorway for IC to the ground state then quenching the reaction channel proceeding through electronically excited states. This justifies the experimental evidence for excitation between 239 and 210 nm, as reported by Sage et al.,[4] and in this work, of exclusive slow CH_3 fragments production.

With 193 nm excitation NMP is still prepared in the S_3 state but above the energy of the crossing with the N−CH_3 dissociative S_4 state. If the excited molecules can reach the S_4 state by a conical intersection then the observation of fast CH_3 fragments becomes again possible: that corresponds to the evidence of the work by Tseng et al.[5] and ours.

From the above discussion, it is clear that at long N−CH_3 distances the S_2 and S_4 states are degenerate. Therefore for the fast dissociation channels starting from S_2 or S_4 the difference in the TKER must equal to the difference in the exciting photon energy, provided that a similar internal energy distribution in the fragments occurs. The available experimental evidence points in this direction.

Even if the final state is in common, the fast reaction channels present both similarities and differences. The observed TKER distribution for the fast fragments is always quite broad. According to Sage et al.,[4] this is the signature of a rather broad distribution of internal energy in the parent fragment. Instead the angular distribution of the fast fragments in the two cases is quite different. In the case of excitation around 240 nm the fragment distribution is reported as isotropic, while for 193 nm excitation we observed a partial anisotropy. We relate this experimental evidence to a different time scale for the direct dissociation process in the two situations. A tentative explanation for this different time scale in the production of the fast CH_3 fragments can be found in the different symmetry for the S_1 and S_3 states (respectively A″ and A′ in the C_s point group) that makes IC to the ground state much easier starting from S_3 than from S_1. The fast IC from the initially prepared S_3 state is also the same argument that we used to explain the quenching of the fast fragment dissociation channel in the low energy excitation regime. That is also consistent with the very low quantum yield for the fast reaction channel for excitation at 193 nm with respect to 243 nm excitation.

The photodissociation of NMP shows features that are strictly related to those observed upon photoexcitation of pyrrole: that demonstrates the very general role played by the $\pi\sigma^*$ states on the photochemistry of aromatic molecules. The most striking difference in the photochemical properties of the two molecules is the existence of two direct dissociation channels, quite close in energy, leading to the production of CH_3 fragments upon photoexcitation of NMP with respect to the single one observed for pyrrole. Simple MO evaluations, supported by TD-DFT calculations, show that stereoelectronic effects due to the coupling between the substituent MOs with the aromatic system are responsible for this difference.

The reaction dynamics schemes we propose for $N-CH_3$ photodissociation in NMP account for the different experimental evidence presented in previous studies[4,5] and in our work, including the existence of the difference reaction channels, changes in the quantum yield for the different reaction channels with excitation energy, and angular distribution of the fragments (that we have measured and reported here for the firts time for 193 nm excitation).

A behavior similar to the one reported for NMP photodissociation along the $N-CH_3$ coordinate should be expected whenever the reaction dynamics of methyl-substituted aromatic molecules is investigated, and we are planning to extend this study on different systems.

Acknowledgment. This research was financially supported by EU under the RII3-CT-2003-506350 program and the Marie-Curie MTKD-CT-2004-509761 Transfer of Knowledge program. The authors wish to thank P.R. Salvi and M. Pasquini (both at Chemistry Dept., Univ. Firenze) for many helpful discussions about the excited states calculations and for assistance with the laser system and the data acquisition system, respectively.

References and Notes

(1) Ashfold, M. N. R.; Cronin, B.; Devine, A. L.; Dixon, R. N.; Nix, M. G. D. *Science* **2006**, *312*, 1637.

(2) Cronin, B.; Nix, M. G. D.; Devine, A. L.; Dixon, R. N.; Ashfold, M. N. R. *Phys. Chem. Chem. Phys.* **2005**, *8*, 599.

(3) Wei, J.; Kuczmann, A.; Riedel, J.; Renth, F.; Temps, F. *Phys. Chem. Chem. Phys.* **2003**, *8*, 315.

(4) Sage, A. G.; Nix, M. G. D.; Ashfold, M. N. R. *Chem. Phys.* **2008**, *347*, 300.

(5) Tseng, C.-M.; Lee, Y. T.; Ni, C.-K. *J. Phys. Chem. A* **2009**, *113*, 3881.

(6) Papadakis, V.; Kitsopoulos, T. N. *Rev. Sci. Instr.* **2006**, *77*, 083101.

(7) Van Vee, G. N. A.; Baller, T.; de Vries, A. E. *Chem. Phys.* **1985**, *92*, 59.

(8) Vallet, V.; Lan, Z.; Mahapatra, S.; Sobolewski, A. L.; Domcke, V. *J. Chem. Phys.* **2005**, *123*, 144307.

(9) Frisch, M. J.; Trucks, G. W.; Schlegel, H. B.; Scuseria, G. E.; Robb, M. A.; Cheeseman, J. R.; Montgomery, J. A., Jr.; Vreven, T.; Kudin, K. N.; Burant, J. C.; Millam, J. M.; Iyengar, S. S.; Tomasi, J.; Barone, V.; Mennucci, B.; Cossi, M.; Scalmani, G.; Rega, N.; Petersson, G. A.; Nakatsuji, H.; Hada, M.; Ehara, M.; Toyota, K.; Fukuda, R.; Hasegawa, J.; Ishida, M.; Nakajima, T.; Honda, Y.; Kitao, O.; Nakai, H.; Klene, M.; Li, X.; Knox, J. E.; Hratchian, H. P.; Cross, J. B.; Adamo, C.; Jaramillo, J.; Gomperts, R.; Stratmann, R. E.; Yazyev, O.; Austin, A. J.; Cammi, R.; Pomelli, C.; Ochterski, J. W.; Ayala, P. Y.; Morokuma, K.; Voth, G. A.; Salvador, P.; Dannenberg, J. J.; Zakrzewski, V. G.; Dapprich, S.; Daniels, A. D.; Strain, M. C.; Farkas, O.; Malick, D. K.; Rabuck, A. D.; Raghavachari, K.; Foresman, J. B.; Ortiz, J. V.; Cui, Q.; Baboul, A. G.; Clifford, S.; Cioslowski, J.; Stefanov, B. B.; Liu, G.; Liashenko, A.; Piskorz, P.; Komaromi, I.; Martin, R. L.; Fox, D. J.; Keith, T.; Al-Laham, M. A.; Peng, C. Y.; Nanayakkara, A.; Challacombe, M.; Gill, P. M. W.; Johnson, B.; Chen, W.; Wong, M. W.; Gonzalez, C.; Pople, J. A. *GAUSSIAN 03*, rev. C02, Gaussian Inc.: Wallingford, CT, 2004.

(10) Sobolewski, A. L.; Domcke, W. *Chem. Phys.* **2000**, *259*, 181.

(11) Zare, R. N. *Mol. Photochem.* **1972**, *4*, 1.

(12) Williamson, A. D.; Miller, J. C.; Compton, R. N. *J. Chem. Phys.* **1980**, *73*, 1527.

(13) Philis, J. G. *J. Mol. Struct.* **2002**, *651−653*, 567.

(14) Biswas, N.; Wategaonkar, S.; Philis, J. G. *Chem. Phys.* **2003**, *293*, 99.

JP903992U